Increased integration between default mode and task-relevant networks in children with ADHD is associated with impaired response control

Kelly A. Duffy [a,1,2], Keri S. Rosch [b,c,d,1], Mary Beth Nebel [b,e], Karen E. Seymour [b,d,f,3], Martin A. Lindquist [g], James J. Pekar [h,i], Stewart H. Mostofsky [b,d,e], Jessica R. Cohen [a,j,k,*]

[a] Department of Psychology and Neuroscience, University of North Carolina at Chapel Hill, Chapel Hill, NC, USA
[b] Center for Neurodevelopmental and Imaging Research, Kennedy Krieger Institute, Baltimore, MD, USA
[c] Department of Neuropsychology, Kennedy Krieger Institute, Baltimore, MD, USA
[d] Department of Psychiatry and Behavioral Sciences, Johns Hopkins University, Baltimore, MD, USA
[e] Department of Neurology, Johns Hopkins University, Baltimore, MD, USA
[f] Department of Mental Health, Bloomberg School of Public Health, Johns Hopkins University, Baltimore, MD, USA
[g] Department of Biostatistics, Bloomberg School of Public Health, Johns Hopkins University, Baltimore, MD, USA
[h] F.M. Kirby Research Center for Functional Brain Imaging, Kennedy Krieger Institute, Baltimore, MD, USA
[i] Department of Radiology and Radiological Science, Johns Hopkins University, Baltimore, MD, USA
[j] Biomedical Research Imaging Center, University of North Carolina at Chapel Hill, Chapel Hill, NC, USA
[k] Carolina Institute for Developmental Disabilities, University of North Carolina at Chapel Hill, Chapel Hill, NC, USA

ARTICLE INFO

ABSTRACT

Default mode network (DMN) dysfunction is theorized to play a role in attention lapses and task errors in children with attention-deficit/hyperactivity disorder (ADHD). In ADHD, the DMN is hyperconnected to task-relevant networks, and both increased functional connectivity and reduced activation are related to poor task performance. The current study extends existing literature by considering interactions between the DMN and task-relevant networks from a brain network perspective and by assessing how these interactions relate to response control. We characterized both static and time-varying functional brain network organization during the resting state in 43 children with ADHD and 43 age-matched typically developing (TD) children. We then related aspects of network integration to go/no-go performance. We calculated participation coefficient (PC), a measure of a region's inter-network connections, for regions of the DMN, canonical cognitive control networks (fronto-parietal, salience/cingulo-opercular), and motor-related networks (somatomotor, subcortical). Mean PC was higher in children with ADHD as compared to TD children, indicating greater integration across networks. Further, higher and less variable PC was related to greater commission error rate in children with ADHD. Together, these results inform our understanding of the role of the DMN and its interactions with task-relevant networks in response control deficits in ADHD.

1. Introduction

Attention-deficit/hyperactivity disorder (ADHD) is a neurodevelopmental disorder characterized by developmentally inappropriate symptoms of inattention, hyperactivity, or impulsivity (American Psychiatric Association, 2013). Deficient response control, including both inhibition errors and inconsistent response speed, is considered a core cognitive deficit of ADHD that may give rise to these symptoms (Barkley, 1997). Indeed, meta-analyses have shown that as compared to typically developing (TD) children, children with ADHD consistently show reduced ability to inhibit motor responses to non-target stimuli (Lijffijt et al., 2005; Willcutt et al., 2005) and increased trial-by-trial variability in response speed (Karalunas et al., 2014; Kofler et al., 2013; Tamm et al., 2012). Conceptually, response in-

---

hibition errors are thought to reflect impulsivity (Bari and Robbins, 2013), whereas response time variability is thought to reflect inconsistent attention (Leth-Steensen et al., 2000; Sergeant, 2005; Castellanos et al., 2005; although for alternative models see: Kofler et al., 2013). However, prevailing models of ADHD suggest that similar neural mechanisms may underlie response inhibition errors and response time variability (Denckla, 1991; Mostofsky and Simmonds, 2008), with prior research demonstrating that they are correlated (Mostofsky and Simmonds, 2008). Yet the neural mechanisms underlying impaired inhibition errors and response variability in ADHD remain unclear.

The default mode network (DMN), which consists of frontal and posterior midline, medial and lateral temporal, and inferior parietal regions (Andrews-Hanna et al., 2010; Raichle et al., 2001), is one possible candidate that is consistently implicated in ADHD (Castellanos and Aoki, 2016; Henry and Cohen, 2019; Konrad and Eickhoff, 2010; Posner et al., 2014). The role of the DMN is thought to be diverse (Andrews-Hanna et al., 2010; Buckner and DiNicola, 2019), with the predominant theory of its role in ADHD purporting that DMN dysfunction may underlie attention lapses (Broyd et al., 2009; Castellanos and Aoki, 2016; Sonuga-Barke and Castellanos, 2007; Weissman et al., 2006). Support for this theory comes from findings that the DMN exhibits maximal activity during internally-oriented thought, with reductions in activity when attention is directed externally. In ADHD, reduced deactivation of DMN brain regions during cognitive tasks is observed, which is associated with greater response time variability (Fassbender et al., 2009) and more omission errors (Helps et al., 2010).

In addition to assessing DMN activation during a task, examining functional connectivity (i.e., correlated activity among different brain regions) between the DMN and task-relevant networks can inform whether DMN intrusions into task-relevant network functioning may underlie attention lapses. Traditionally, a single measure of functional connectivity averaged across an fMRI run, or static functional connectivity, is investigated. Previous static functional connectivity analyses report atypical DMN connectivity in ADHD, including both within-network connections (Fair et al., 2010; Kessler et al., 2014; Sripada et al., 2014; Sun et al., 2012) and connections between the DMN and task-relevant networks (Kessler et al., 2014; Mills et al., 2018; Sripada et al., 2014; Sun et al., 2012). However, examining changes in functional connectivity patterns within an fMRI run, or time-varying functional connectivity, may be a particularly relevant indicator of network dysfunction in ADHD, given that variability in behavior and attention across time is commonly experienced by individuals with ADHD (Castellanos et al., 2005; Karalunas et al., 2014; Leth-Steensen et al., 2000).

Studies in healthy young adults have reported that the strength of interactions between the DMN and attention-related networks varies across time (Dixon et al., 2017) and that momentary increases in integration between the DMN and regions of task-relevant networks are associated with behavioral indices of inattention, including missed stimuli during stimulus detection (Sadaghiani et al., 2015) and increased response time variability during finger-tapping (Kucyi et al., 2017). Thus far, the studies that have assessed time-varying functional connectivity in ADHD provide support for the theory that altered DMN-related dynamics are relevant to ADHD, although the direction of findings is inconsistent. Some studies have reported restricted, or less dynamic, DMN functional connectivity in ADHD as compared to TD individuals. This holds for within-DMN connections (de Lacy and Calhoun, 2019), as well as connections between the DMN and sensory networks (Wang et al., 2018), and between the DMN and higher-order task-relevant networks (Abbas et al., 2019). Other literature, however, suggests that interactions between the DMN and task-relevant networks are more dynamic in ADHD as compared to TD individuals (Cai et al., 2018; Kaboodvand et al., 2020). When modeling the sequence of functional connectivity patterns between the DMN and task-relevant networks (i.e., brain states) throughout the resting state, it has been found that children with ADHD are less likely to enter

into or maintain brain states characterized by anticorrelations between the DMN and task-relevant networks (Shappell et al., 2021). Finally, altered dynamics between the DMN and task-relevant networks have been found to be correlated with ADHD symptoms (Cai et al., 2018) and cognitive control performance in adults (i.e., Stroop incongruent reaction times; Kaboodvand et al., 2020). Together, these findings broadly support the Default Mode Interference Hypothesis (Sonuga-Barke and Castellanos, 2007), which proposes that regular, dynamic fluctuations between the DMN and task-relevant regions are disrupted in ADHD due to increased DMN interactions with task-relevant networks. Further research examining features of network topology and how they relate to behavioral indicators of response control among children with ADHD may help clarify these inconsistent findings, which largely focus on the strength of functional connections.

The goal of the current study, therefore, is to use a network perspective to examine how DMN integration with task-relevant cognitive control networks (fronto-parietal [FP] and salience/cingulo-opercular [SAL]) and motor networks (hand somatomotor [SM] and subcortical [SUB]) during the resting state relates to poor response control during a go/no-go (GNG) task in children with ADHD. We aim to extend research focusing on functional connectivity strength to understand how altered functional connectivity impacts overall network topology, both from a static and from a time-varying perspective. To assess time-varying functional connectivity we implement the dynamic conditional correlation (DCC) method, a model-based approach that estimates functional connectivity at each timepoint by constructing time-series that consist of a weighted combination of past timepoints. The DCC method was selected instead of the commonly-implemented sliding window approach because it has been shown to more reliably distinguish true dynamic signal from noise (Choe et al., 2017). As we are specifically interested in integration across brain networks, we focus our analyses on participation coefficient (PC), a metric that quantifies the degree to which a node is connected across networks in a graph. To determine whether our results are specific to across-network integration, in post hoc exploratory analyses we additionally assess within-module degree (WD), a metric that quantifies the strength of a node's connections within its own network. We hypothesize that increased DMN integration with both cognitive control and motor networks, as well as restricted network dynamics across these networks, will be observed in children with ADHD and will relate to poor response control (i.e., increased inhibition errors and higher response time variability) during a GNG task. Given the findings in ADHD of a relationship between increased DMN activity and poor task performance (Fassbender et al., 2009; Helps et al., 2010), as well as dysfunctional DMN connectivity with other brain networks (Castellanos and Aoki, 2016; Henry and Cohen, 2019; Konrad and Eickhoff, 2010; Posner et al., 2014), we focus our analyses on interactions between the DMN and each of the other networks. We further hypothesize that our results will be specific to DMN integration with other networks, and thus will not extend to within-network connectivity strength. This research has the potential to enhance understanding of how intrusions of the DMN into task-relevant network functioning may contribute to impaired response control in children with ADHD.

2. Methods

2.1. Participants

Participants included 143 children with ADHD and 133 TD children aged 8–12 years who completed both a resting state fMRI scan and a GNG task outside of the scanner. One hundred children with ADHD were excluded for the following reasons: a sibling in the study ($n = 1$), cortical signal loss ($n = 2$), or excessive motion during the resting state scan ($n = 97$), leaving 43 children with ADHD (mean age 10.26, 13 girls) for analysis. Eighty TD children were excluded for the following reasons: a sibling in the study ($n = 7$) or excessive motion during the

resting state scan (n = 73), leaving 53 TD children. See *fMRI Data Processing* for specific motion-related exclusion criteria. Among the TD children, we pseudo-randomly selected 43 as comparison participants (mean age 10.18, 14 girls), with the constraint that the groups be matched for age, sex, IQ, and socioeconomic status. We note that we applied strict motion criteria because functional connectivity analyses in general, and time-varying functional connectivity analyses in particular, are highly susceptible to motion artifacts. We were thus conservative in our inclusion criteria to increase the likelihood of non-artifactual results. Notably, potential participants who were excluded for motion did not significantly differ in age, sex, ADHD symptom severity, or GNG task performance from participants who were included (all p-values > .20). Participant demographics, clinical characteristics, behavioral task performance data, and in-scanner head motion are summarized in Table 1.

Participants were primarily recruited through local public schools, with additional resources including community-wide advertisements, volunteer organizations, medical institutions, and word of mouth. This study was approved by the Johns Hopkins University School of Medicine Institutional Review Board. Written consent was obtained from the parent/guardian and assent was obtained from the participating child.

Phone screens were conducted to assess initial eligibility and exclude children with a history of intellectual disability, seizures, traumatic brain injury or other neurological illnesses, documented psychiatric diagnosis (other than ADHD or oppositional defiant disorder for ADHD participants), current psychoactive medication except short-acting stimulant medication (ADHD participants only), an immediate family member with ADHD (TD participants only), and MRI contraindications. Final study eligibility was determined based on: (1) a psychiatric diagnostic interview with the parent/caregiver using either the Diagnostic Interview for Children and Adolescents, Fourth Edition (DICA-IV; Reich et al., 1997) for participants enrolled before February 2015 or the Kiddie Schedule for Affective Disorders and Schizophrenia for School-Aged Children-Present and Lifetime Version (K-SADS-PL; Kaufman et al., 2013) for all other participants; (2) an intellectual and academic skills assessment using the Wechsler Intelligence Scale for Children, Fourth or Fifth Edition (WISC-IV or WISC-V; Wechsler, 2003, 2014) to determine the full scale intelligence quotient (FSIQ) and general ability index (GAI), as well as the Word Reading subtest of the Wechsler Individual Achievement Test, Second or Third Edition (WIAT-II or WIAT-III; Wechsler, 2002, 2009) to screen for a reading disorder; and (3) completion of rating scales of ADHD symptoms using the Conners' Parent or Teacher Rating Scales-Revised or the Conners-3 (Conners, 2002, 2008). See Table 1 for a break-down of the number of participants who received each assessment.

For inclusion in the ADHD group, children had to meet full DSM-IV or DSM-5 criteria for ADHD based on the following: (1) an ADHD diagnosis according to the diagnostic interview; and (2) a T-score of 65 or higher on the Conners' Parent or Teacher (when available) DSM Inattentive Type and/or DSM Hyperactive/Impulsive Type scales. Master's level clinicians conducted all diagnostic interviews and collected all rating scales under the supervision of licensed clinical psychologists. All information was reviewed and diagnoses confirmed by a child neurologist (S.H.M.) or licensed clinical psychologist (K.S.R. or K.E.S.). Children were excluded for FSIQ scores below 80 on the WISC-IV/V or Word Reading scores from the WIAT-II/III below 85. ADHD and TD groups were matched on the GAI of the WISC-IV/V. Children with ADHD on short-acting stimulant medication were eligible to participate if they withheld medication the day prior to and day of testing.

Participants completed two days of testing. On the first day, they completed the GNG task and a mock scan to prepare them for the scanner environment. On the second day, they completed the MRI scan.

2.2. GNG task

Participants completed a GNG task outside of the fMRI scanner on the first day of testing. Task stimuli included green spaceships for "go" trials (80%) or red spaceships for "no-go" trials (20%) presented one at a time. Participants were instructed to push the spacebar with their index finger as quickly as possible for green spaceships and to withhold their response for red spaceships. Trial order was pseudo-random, with the constraint that there were never fewer than three go trials before a no-go trial. There were 11 practice trials followed by 217 experimental trials. Stimuli were displayed on the screen for 300 ms, with an interstimulus interval of 2000 ms (fixation cross). Behavioral metrics quantifying response inhibition (ComErr: commission error rate, or failures to inhibit on no-go trials) and response variability (tau: the exponential component of the response time distribution) were calculated. We calculated tau as our measure of response variability based on studies showing that relatively infrequent, very slow response times (represented by the tau parameter of an ex-Gaussian function) primarily contribute to increased response variability in ADHD (Karalunas et al., 2014; Kofler et al., 2013). Tau was computed by fitting an ex-Gaussian function to each participant's go response times using the DISTRIB toolbox in MATLAB (Lacouture and Cousineau, 2008). As tau is not normally distributed (Shapiro–Wilk test of normality = 0.78, p = 5.9E−10), we transformed tau using the natural logarithm (transformed tau Shapiro–Wilk test of normality = 0.98, p = .15) and conducted all analyses using the log-transformed tau.

2.3. fMRI data acquisition

Imaging data were collected using either an 8-channel (n = 31) or 32-channel (n = 53) head coil (n = 2 unknown) with a 3-Tesla Philips Achieva whole-body MR machine at the Kennedy Krieger Institute F. M. Kirby Research Center for Functional Brain Imaging. Whole-brain functional data were acquired during the resting state using a multi-slice SENSE-EPI pulse sequence (TR = 2500 ms, TE = 30 ms, SENSE factor = 2, flip angle = 70°, 47 contiguous ascending 3 mm slices with an in-plane resolution of 3.05 mm x 3.15 mm). Participants were instructed to stay awake with their eyes open and to fixate on a white crosshair in the center of a gray screen. Participants received a single resting state run that lasted between 5.3 min (128 volumes; n = 6) and 6.5 min (156 volumes; n = 80). A high-resolution T1-weighted structural 3D MP-RAGE was also acquired (TR = 8 ms, TE = 3.7 ms, flip angle = 8°, resolution = 1 mm x 1 mm x 1 mm). Additional scans, not relevant to this set of analyses, were also collected in a subset of the participants and will not be discussed here.

2.4. fMRI data processing

Functional data were first minimally preprocessed using FMRIPREP version 1.0.7 (Esteban et al., 2019). Briefly, preprocessing of the T1-weighted image included intensity nonuniformity correction, skull-stripping, spatial normalization to the ICBM 152 Nonlinear Asymmetrical template version 2009c (Fonov et al., 2009), and segmentation. Preprocessing of the functional data included slice time correction, motion correction, and co-registration to the T1-weighted image. For details of the FMRIPREP preprocessing, see *Supplementary Material*.

Following the minimal preprocessing by FMRIPREP, data were further processed using two methods, one that scrubbed motion-contaminated timepoints for static connectivity analyses and one that did not scrub any data for time-varying functional connectivity analyses. For the data that were scrubbed, all timepoints with framewise displacement (FD; Power et al., 2014) greater than 0.25 mm were replaced using spectral interpolation (Carp, 2013; Ciric et al., 2017). Following spectral interpolation for scrubbed time-series, and following FMRIPREP minimal preprocessing for unscrubbed time-series, both data and nuisance regressors were bandpass filtered (0.01–0.8 Hz) as per current recommendations (Lindquist et al., 2019),

Table 1
Demographic information and behavioral performance.

	ADHD (n = 43)	TD (n = 43)	p-values (FDR-corr)
Age (yrs)	10.26 (1.36)	10.18 (0.96)	.82
Sex (M/F)	30 / 13	29 / 14	.82
SES	54.43 (8.39)	54.99 (8.25)	.52
GAI	112.57 (15.66)	117.74 (12.20)	.14
% ODD diagnosis	30.23%	0%	.0001*
ADHD Inattention T-Score[a]	73.16 (10.86)	46.05 (5.81)	6.4E−21*
ADHD Hyperactivity/Impulsivity T-Score[a]	69.58 (15.18)	46.81 (5.20)	4.0E−12*
% taking stimulant medication	67.44%	0%	N/A
Motion during resting state scan: FD (mm)	0.15 (0.06)	0.11 (0.03)	.00018*
GNG Commission Error Rate	0.46 (0.20)	0.38 (0.17)	.033*
GNG Tau, log-transformed (ms)	4.74 (0.55)	4.49 (0.47)	.033*

All results are presented as Mean (SD), or % when specified. FD = framewise displacement. GAI = General Ability Index on the WISC-IV (n = 70; Wechsler, 2003) or WISC-V (n = 16; Wechsler, 2014). GNG = go/no-go. ODD = oppositional defiant disorder. Diagnoses confirmed using either the DICA-IV (n = 65; Reich et al., 1997) or KSADS-PL (n = 21; Kaufman et al., 2013). SES = socioeconomic status of parents (Hollingshead, 1975). Tau = the exponential component of the response time distribution; reported values are log-transformed.
[a]T-scores from Conners Parent Rating Scales-Revised (n = 41; Conners, 2002) or Conners-3 (n = 45; Conners, 2008) DSM inattention and hyperactivity/impulsivity subscales.
*= significant group difference using Welch's t-tests for unequal variance (or, in the case of sex and comorbid diagnoses, two-sample chi-squared test), FDR-corrected p < .05.

and 32-parameter nuisance regression was applied (6 rigid body motion parameters, mean cerebrospinal fluid, and mean white matter; temporal derivatives and quadratic expansions of these 8 regressors; quadratic expansions of the 8 temporal derivatives). For the data that were scrubbed, an additional step was next taken to remove all timepoints with FD greater than 0.25 mm, with the criterion that 5 contiguous timepoints were required between each scrubbed timepoint to minimize the contamination of longer epochs of motion (Power et al., 2014). These steps were chosen based on the best-performing artifact removal procedures as described by Ciric and colleagues (2017) and Parkes and colleagues (2018).

Participants were excluded for excessive motion if their mean FD was greater than 0.25 mm, if 40% or more of their data was removed using the scrubbing criteria described above, or if less than 4 min of data remained after scrubbing (Parkes et al., 2018; Van Dijk et al., 2010). As reported in Table 1, participants with ADHD had significantly higher mean raw FD (i.e., before motion correction) than TD participants (Welch's t-test for unequal variances: t(67.14) = 4.32, uncorrected p < .0001, mean ADHD = 0.15 mm, mean TD = 0.11 mm). We chose to not match the groups on mean FD given evidence that head motion is correlated with ADHD symptomatology and that head motion and ADHD may have similar genetic loadings (Couvy-Duchesne et al., 2016). Thus, matching groups on mean FD may result in a non-representative sample of children with ADHD. See *Supplementary Material* for analyses showing that mean raw FD was correlated with ADHD symptoms and GNG task performance in our sample and for additional analyses to confirm that we properly controlled for motion in our data processing. Briefly, we quantified recommended quality control metrics (Ciric et al., 2017, 2018) to ensure that the quality of the data was sufficient and comparable across groups. Additionally, we replicated results implementing four different methods controlling for motion to ensure that our results were robust to participant motion: (1) including mean FD as an additional covariate in all analyses; (2) including DVARS (i.e., the change in BOLD signal across time) as an additional covariate in all analyses; (3) using unscrubbed, as opposed to scrubbed, data; and (4) using a motion-matched sample of participants. Results, reported in detail in the *Supplementary Material*, demonstrated that our findings were largely consistent across all methods used to control for participant motion.

2.5. Functional connectivity

To calculate functional connectivity between pairs of brain regions, we partitioned the brain into 157 10 mm diameter spherical cortical and subcortical regions of interest (ROIs) using networks of interest

from a commonly-used functional brain atlas (Power et al., 2011; Fig. 1). We selected networks found to be dysfunctional in ADHD (Cao et al., 2014; Castellanos and Proal, 2012; Henry and Cohen, 2019): the default mode (DMN; 57 regions that had brain coverage in our participants; 1 ROI was excluded for lack of coverage), fronto-parietal (FP; 25 regions), salience/cingulo-opercular (SAL; 32 regions), hand somatomotor (SM; 30 regions), and subcortical (SUB; 13 regions) networks. The fully processed time-series data were averaged within each ROI.

For static functional connectivity analyses, scrubbed time-series were used. Each ROI's average scrubbed time-series was correlated with the average scrubbed time-series for all other ROIs, resulting in a 157 x 157 correlation matrix for each participant. The correlation coefficients were Fisher-transformed into z-scores in order to allow for statistical conclusions to be made from the magnitudes of the correlations.

For time-varying functional connectivity analyses, the dynamic conditional correlation (DCC) method was applied to the unscrubbed time-series, as temporal contiguity is necessary to assess functional connectivity changes across time. The DCC method is a multivariate volatility model based on a generalized autoregressive conditional heteroscedastic approach. It computes the conditional covariance between all pairs of ROIs at a given timepoint based on a weighted combination of past values, with a variable window length determined using a quasi-maximum likelihood approach. It is similar to autoregressive models commonly used to estimate noise in fMRI data. This is in contrast to traditional sliding window approaches, which use set window lengths and either weight all values equally or taper weights according to a function regardless of prior behavior of the time-series. For more details on the method and its increased reliability in separating true time-varying functional connectivity from noise as compared to sliding window approaches, see Lindquist et al. (2014) and Choe et al. (2017). We constructed 157 x 157 functional connectivity matrices for each volume, discarding the first 5 and last 5 volumes to allow the model to stabilize. Therefore, each participant had either 118 or 146 time-varying FC matrices depending on the length of their resting state scan. Finally, as in the static functional connectivity analyses, the correlation coefficients for each volume were Fisher-transformed. The DCC functional connectivity matrices were used in subsequent graph analyses (see below).

2.6. Graph construction and metrics

Undirected, weighted graphs were constructed from the Fisher-transformed correlation matrices described above. All negative correlation values were set to 0. Graph metrics were then calculated using the
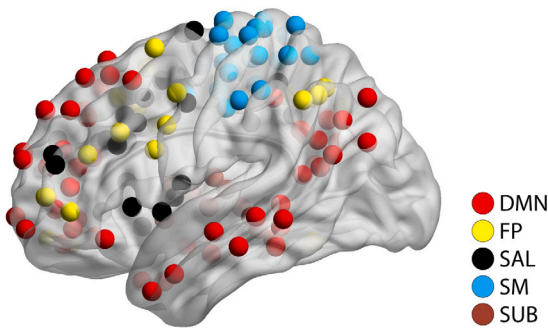
Fig. 1. Regions of interest (ROIs) from the default mode network (DMN), fronto-parietal network (FP), combined salience/cingulo-opercular networks (SAL), hand somatomotor network (SM), and subcortical network (SUB). ROIs taken from Power et al. (2011).

Brain Connectivity Toolbox (www.brain-connectivity-toolbox.net; Rubinov and Sporns, 2010). For static connectivity analyses, a single graph was constructed per run for each participant. For time-varying connectivity analyses, one graph per timepoint was constructed, resulting in either 118 or 146 graphs for each participant (depending on initial number of timepoints collected; see *fMRI Data Acquisition*).

Because we were interested in the degree of integration across networks, we used the predefined network assignments of the functional atlas and calculated participation coefficient (PC; Guimerà and Amaral, 2005a,b). PC quantifies the distribution of a node's inter-network, or inter-module, connections, such that a PC of 1 indicates that the node has equally distributed connections to all other modules (i.e., high inter-network integration), while a PC of 0 indicates that all of a node's connections are within its own module (i.e., low inter-network integration). For weighted graphs, PC is defined as:

$$PC_i = 1 - \sum_{s=1}^{N_m} \left(\frac{k_i^w(s)}{k_i^w}\right)^2 \qquad (1)$$

where N_M is the number of modules, $k_i^w(s)$ is the weighted connections between node i and nodes in module s, and k_i^w is the total weighted connections of node i, regardless of module (Rubinov and Sporns, 2010). As PC is a nodal metric, the mean across all nodes was taken to get a single value of the average PC of each graph. To examine connections between pairs of networks, we calculated PC for subgraphs consisting of the DMN and each other network (e.g., between the DMN and FP networks). Exploratory analyses of interactions between all other pairs of networks are presented in the *Supplementary Material*, as are additional analyses probing differential integration between DMN subnetworks and each of the task-relevant networks. For static analyses, a single PC value was computed for the whole network and for each network pair for each participant. For time-varying analyses, a vector of PC values was computed for the whole network, with each PC value corresponding to a single timepoint of the resting state scan. Coefficient of variation (standard deviation/mean) of PC (CVPC) was calculated as the metric of interest to account for potential group differences in static PC. Specifically, standard deviation across all PC values was calculated for each node then averaged across all nodes to get a single value for each participant of the standard deviation of PC of each graph. This value was divided by mean PC as calculated from the static FC analyses, resulting in a single value of CVPC for each participant.

To assess whether any group differences or relationships with behavior were specific to network integration, in exploratory analyses we calculated within-module degree (WD; Guimerà and Amaral, 2005a,b), a measure that quantifies how highly connected a given node is to other nodes within its module. For weighted graphs, WD is often a standardized metric (a z-score); however, since our analyses involve averaging across nodes, which would result in a value of 0 for standardized nodal

WD values, we do not standardize WD. Thus, the WD of a given node is simply defined as:

$$z_i^w = k_i^w(m_i) \qquad (2)$$

where m_i is the module containing node i, and $k_i^w(m_i)$ is the number of connections between node i and all other nodes in module m_i (i.e., the weighted degree of node i within its own module). Similar to PC analyses, the mean WD across all nodes was calculated to get a single value for each participant of the average, whole-network WD. To examine connections within each network separately, nodal WD was additionally averaged within each individual network (e.g., within the DMN or within the FP network). Finally, in time-varying analyses coefficient of variation of WD (CVWD) was calculated at the whole-network level in a manner identical to the calculation of CVPC.

2.7. Analyses

Welch's t-tests for unequal variance were conducted to compare behavioral performance across groups. As mean functional connectivity strength (average of all edges) has been shown to impact graph metric calculations (van den Heuvel et al., 2017), which was the case in our sample (all false discovery rate [FDR]-corrected p-values for correlations between mean functional connectivity and neural metric outcomes of interest < 1E-7), all analyses involving neural data control for the effect of mean functional connectivity. We additionally controlled for age, as age was correlated with GNG performance in our sample ($r = -0.20$, corrected $p = .064$ for ComErr and $r = -0.34$, corrected $p = .003$ for tau, FDR-corrected for two comparisons). One-way ANCOVAs with group as the factor and mean functional connectivity and age as the covariates were conducted to compare mean PC and CVPC across groups. Pearson's correlations (partial correlations controlling for mean functional connectivity and age) were conducted to relate graph metrics to performance on the GNG task, separately for each group. All statistical tests were corrected for multiple comparisons using an FDR correction as follows. We corrected t-tests comparing behavioral metrics across groups for two comparisons (tau, ComErr), within-group correlations relating whole network neural metrics with behavior for two comparisons each (tau, ComErr), and planned DMN network pair static PC ANCOVAs and within-group correlations for four comparisons each (DMN-FP, DMN-SAL, DMN-SM, DMN-SUB).

Exploratory WD analyses were similarly conducted. First, one-way ANCOVAs with group as the factor and mean functional connectivity and age as the covariates were conducted to compare mean WD and CVWD across groups. Next, Pearson's correlations (partial correlations controlling for mean functional connectivity and age) were conducted to relate WD to performance on the GNG task, separately for each group. Within-group correlations relating whole network neural metric with behavior were FDR-corrected for two comparisons each (tau, ComErr) and single network static WD ANCOVAs and within-group correlations were corrected for five comparisons each (DMN, FP, SAL, SM, SUB).

3. Results

3.1. GNG behavioral performance

Compared to TD children, children with ADHD showed poorer response inhibition (ComErr: $t(82.1) = 2.17$, corrected $p = .033$) and increased response variability on Go trials (tau: $t(82.1) = 2.19$, corrected $p = .033$). See Table 1 for descriptive statistics.

Table 2

Mean participation coefficient (PC) for ADHD and TD participants.

Networks	ADHD	TD	Group difference	
			F-value (df=1,78)	p-value (FDR-corr)
Whole-network	0.717	0.709	4.08	.046*
DMN-FP	0.374	0.358	8.81	.016*
DMN-SAL	0.381	0.372	1.53	.292
DMN-SM	0.383	0.383	0.001	.977
DMN-SUB	0.252	0.242	3.34	.143

Group difference ANCOVAs covarying for mean functional connectivity and age. Whole-network includes DMN, FP, SAL, SM and SUB networks. All p-values are FDR-corrected for multiple comparisons.

*= significant ($p < .05$).

3.2. Static functional connectivity

Across all five networks (DMN, FP, SAL, SM, SUB) we observed that mean PC was higher in children with ADHD than in TD children (mean ADHD: 0.717, mean TD: 0.709, $F(1,78) = 4.08$, $p = .047$; Table 2; Fig. 2a). Next, we compared group differences in mean PC between the DMN and each other network to test our hypotheses regarding atypical DMN integration with other networks in ADHD. We found that PC between the DMN and FP networks was significantly higher in ADHD as compared to TD participants (mean ADHD: 0.374, mean TD: 0.358, $F(1,78) = 8.81$, corrected $p = .016$; Table 2; Fig. 2b). No other network pair showed a group difference (all corrected p-values > .14; Table 2).

Given the significant group differences in performance on the GNG task, we next correlated PC across all five networks with ComErr and tau separately for each of the groups. In participants with ADHD, we found that there was a positive correlation between PC and ComErr ($r = 0.35$, corrected $p = .049$), while PC was not correlated with tau ($r = -0.05$, corrected $p = .77$). There were no significant relationships between PC and behavior in TD participants (ComErr: $r = -0.13$, corrected $p = .80$; tau: $r = -0.05$, corrected $p = .80$; Fig. 2c). The relationship between PC and ComErr was significantly stronger in participants with ADHD than in TD participants ($z = 2.23$, $p = .025$).

Given the significant association between PC and ComErr across all five networks in participants with ADHD, we then examined correlations of individual pairwise PC values with ComErr. Findings revealed that among children with ADHD, PC values for DMN-SAL ($r = 0.36$, corrected $p = .043$) and DMN-SM ($r = 0.38$, corrected $p = .043$; Fig. 2d) were positively correlated with ComErr. There were no significant relationships between DMN-FP or DMN-SUB PC and ComErr in the ADHD group (both corrected p-values > .14). Similar to the results averaged across all five networks, these relationships did not hold in the TD participants (all corrected p-values > .37). The relationships between DMN-SAL and DMN-SM PC and ComErr were stronger in the ADHD than in the TD participants (DMN-SAL trend: $z = 1.92$, $p = .055$; DMN-SM significant: $z = 2.98$, $p = .003$).

We additionally conducted two sets of exploratory analyses comparing PC and relationships with behavior across groups. First, we examined interactions between the other networks (e.g., FP-SM PC) to determine whether findings were specific to DMN integration. Second, we divided the DMN into subnetworks to determine whether distinct DMN subnetworks interacted differentially with task-relevant networks. See *Supplementary Material* for results of these analyses.

Finally, to determine whether these findings were specific to across-network integration, we assessed WD, a measure of within-network connectivity strength. Similar to PC, across all five networks we observed that mean WD was higher in children with ADHD than in TD children (mean ADHD: 8.788, mean TD: 8.362, $F(1,78) = 6.45$, $p = .013$). There were no significant group differences when assessing each network separately (all corrected p-values > .11). Similarly, when correlating whole-network WD with ComErr and tau there were no significant relationships with behavior for either participants with ADHD

(ComErr: $r = -0.29$, corrected $p = .13$; tau: $r = 0.04$, corrected $p = .80$) or TD participants (ComErr: $r = 0.15$, corrected $p = .68$; tau: $r = 0.07$, corrected $p = .68$). Finally, there were no correlations with ComErr at the individual network level (all corrected p-values > .12 for ADHD and > .55 for TD). See Table 3 for details.

3.3. Time-varying functional connectivity

Next, we investigated whether variability of functional network organization across time was different across the groups or correlated with GNG performance using CVPC. Here, we focused on whole-network integration (DMN-FP-SAL-SM-SUB). We did not observe a group difference in CVPC across the resting state scan (mean ADHD: 0.037, mean TD: 0.039, $F(1,78) = 1.24$, $p = .27$; Fig. 3a). However, when relating CVPC to response control, we found that in participants with ADHD, CVPC was negatively correlated with ComErr ($r = -0.41$, corrected $p = .015$). CVPC was not correlated with tau in participants with ADHD ($r = -0.05$, corrected $p = .75$). In TD participants, CVPC was not correlated with ComErr ($r = 0.09$, corrected $p = .58$) or with tau ($r = 0.10$, corrected $p = .58$; Fig. 3b). Once again, the relationship between CVPC and ComErr was significantly stronger in participants with ADHD than in TD participants ($z = 2.34$, $p = .019$).

It is possible that a less flexible, integrated network organization leads to higher ComErr in participants with ADHD. In support of this, in a post-hoc analysis we found that the static functional connectivity mean PC across the five networks of interest was highly negatively correlated with the standard deviation of PC in participants with ADHD ($r = -0.90$, $p = 3E$-16). This indicates that greater network integration was associated with less variable (more stable) network structure. This relationship held in TD participants as well ($r = -0.86$, $p = 1E$-13). Notably, we found that more variance was explained in a regression model predicting ComErr in the ADHD participants with CVPC, mean functional connectivity, and age as predictors (adjusted $R^2 = 0.21$, $F(3,39) = 4.62$, $p = .007$) than with mean PC, mean functional connectivity, and age as predictors (adjusted $R^2 = 0.17$, $F(3,39) = 3.82$, $p = .017$).

To probe the specificity of these results to across-network integration, we additionally quantified group differences and correlations with behavior in whole-network CVWD. We found no group difference in CVWD across the resting state scan (mean ADHD: 0.205, mean TD: 0.200, $F(1,78) = 1.66$, $p = .20$). We also found no significant correlations between CVWD and performance on the GNG task in either group. CVWD was not correlated with GNG ComErr (ADHD: $r = 0.32$, corrected $p = .088$; TD: $r = -0.09$, corrected $p = .75$) or GNG tau (ADHD: $r = -0.04$, corrected $p = .80$; TD: $r = -0.05$, corrected $p = .75$) in either participants with ADHD or TD participants.

3.4. Summary of sensitivity analysis findings

To determine whether our results were robust to the method used to control for subject motion, we repeated the above analyses controlling for motion in different ways. We found that results were consistent across all methods implemented, particularly when controlling for FD and DVARS. Not surprisingly, when using unscrubbed data results did not significantly change but effects were reduced, likely due to increased noise and susceptibility to motion artifacts (Ciric et al., 2017; Parkes et al., 2018). When using a motion-matched sample of participants ($n = 29$ per group) group differences did not remain consistent, a change that could have been due to including a non-representative sample of children with ADHD. Correlations with behavior, while no longer significant, were stronger in magnitude in this reduced sample, with the reduced significance likely due to the 33% reduction in sample size. Critically, no results significantly changed from those reported above regardless of the method of controlling for subject motion (all uncorrected p-values > .23). For more details of these analyses, see *Supplementary Material* section 3, "Motion-Related Quality Assurance".
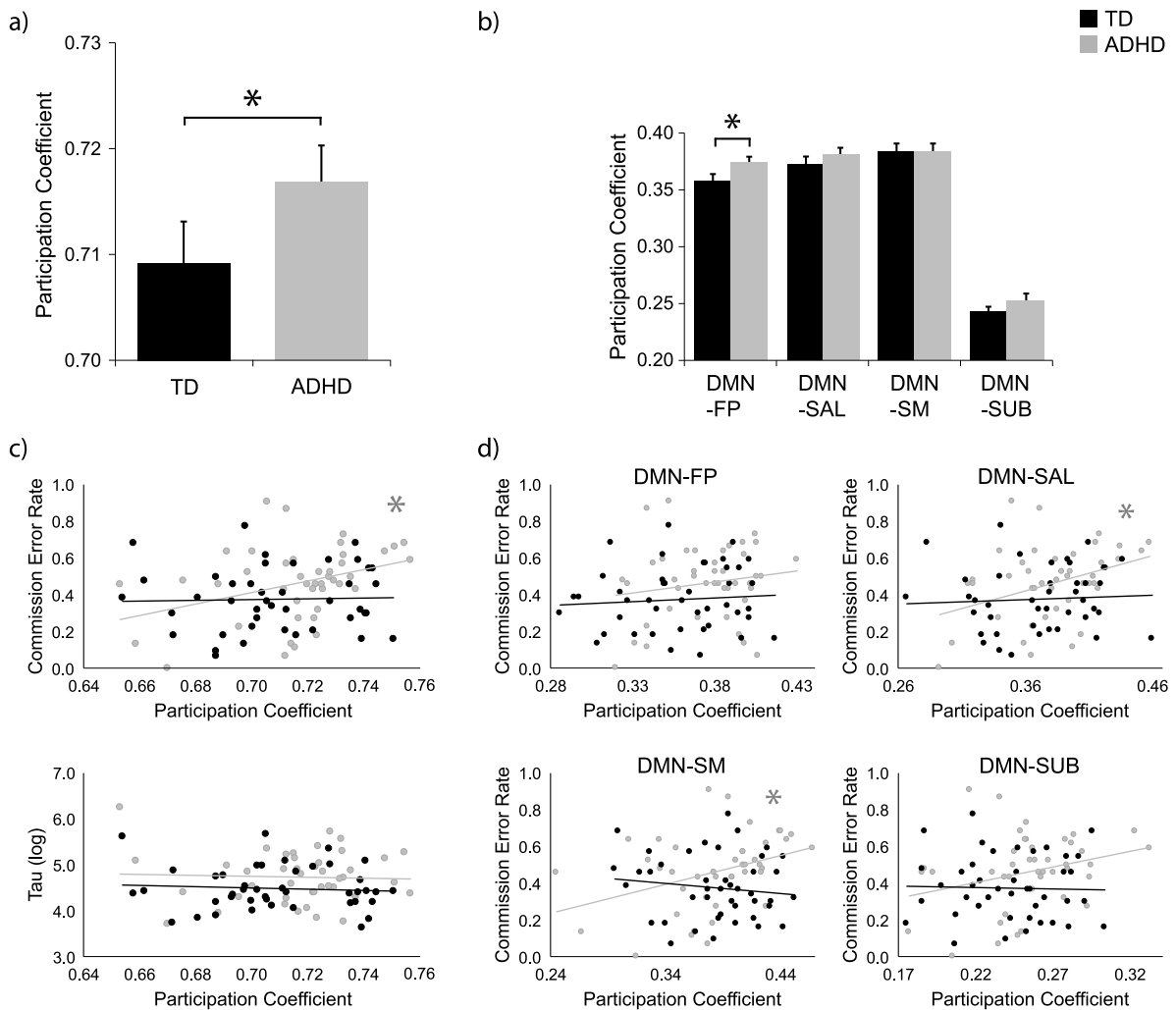
Fig. 2. (a) Significant group difference in participation coefficient (PC) across all five networks (p = .046). (b) Group difference in PC separately for each DMN network pair. There was a significant group difference between the DMN and FP networks (corrected p = .016). (c) Relationships between PC and performance on the go/no-go (GNG) task across all five networks (commission error rate [ComErr; top] and log-transformed tau [bottom]). There was a significant positive correlation between PC and ComErr in ADHD participants (FDR-corrected p = .049). There were no PC-behavior relationships with tau or in the TD participants (all FDR-corrected p-values > .76). (d) Relationships between PC and ComErr separately for each DMN network pair. There were significant positive correlations between DMN-SAL PC and DMN-SM PC and ComErr in the participants with ADHD (both FDR-corrected p-values = .043). There were no relationships between PC and ComErr in the TD participants (all FDR-corrected p-values > .37). * indicates a relationship is significant at FDR-corrected p < .05.

Table 3
Mean within-module degree (WD) and correlations with commission errors (ComErr) for ADHD and TD participants.

Networks	ADHD	TD	Group difference		Correlations	
			F-value (df=1,78)	p-value (FDR-corr)	ADHD ComErr r (FDR-corr p)	TD ComErr r (FDR-corr p)
Whole-network	8.79	8.36	6.45	.013*	−0.29 (.126)	0.15 (.685)
DMN	13.40	12.69	2.41	.208	−0.07 (.816)	0.15 (.559)
FP	5.30	5.52	0.88	.439	−0.35 (.122)	0.19 (.559)
SAL	6.80	6.77	0.006	.938	−0.27 (.217)	0.04 (.786)
SM	7.68	6.77	4.34	.102	−0.11 (.816)	−0.14 (.559)
SUB	2.76	2.47	5.17	.102	0.03 (.864)	−0.12 (.559)

Group difference ANCOVAs and partial correlations covarying for mean functional connectivity and age. Whole-network includes DMN, FP, SAL, SM and SUB networks. All p-values are FDR-corrected for multiple comparisons.
*= significant (p < .05).

4. Discussion

In this study, we related both static and time-varying measures of integration between the DMN and task-relevant networks to performance on a GNG task, including failures of response inhibition (ComErr) and response time variability (tau), in children with ADHD and TD children. On a whole-network level, static connectivity analyses revealed increased integration (i.e., higher PC) between the DMN and task-relevant networks in children with ADHD, with a significant group difference of individual network pairs limited to integration between the DMN and the FP cognitive control network. Notably, for children with ADHD, we additionally found that increased DMN integration with the SAL and SM networks was correlated with increased response inhibition failures on the GNG task. Finally, for children with ADHD,
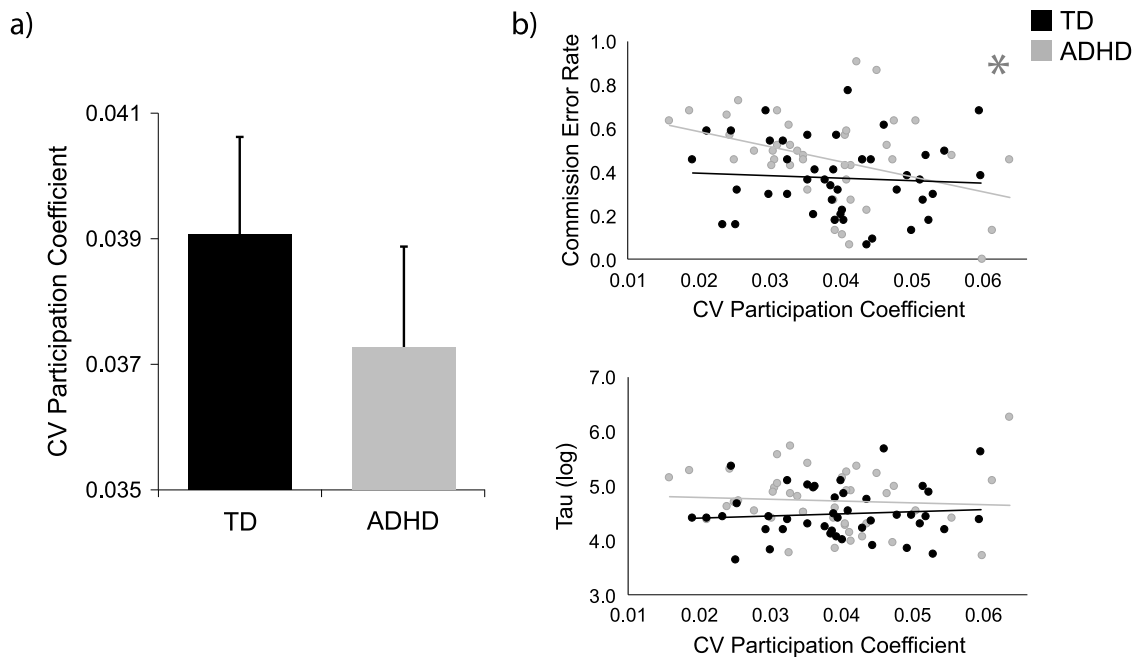
Fig. 3. Across all five networks, a) group difference in coefficient of variation of participation coefficient (CVPC) and b) relationships between CVPC and performance on the go/no-go (GNG) task (commission error rate [ComErr; top] and log-transformed tau [bottom]). There was no group difference in whole-network CVPC. There was a significant negative correlation between CVPC and ComErr in the participants with ADHD (FDR-corrected p = .015). There were no CVPC-behavior relationships with tau or in the TD participants (all FDR-corrected p-values > .57). CV = coefficient of variation. * indicates a relationship is significant at FDR-corrected p < .05.

time-varying connectivity analyses revealed that reduced variability of integration (i.e., lower CVPC) between the DMN and task-relevant networks was correlated with increased response inhibition failures. Additionally, exploratory analyses quantifying within-network coherence (WD) revealed increased static WD on a whole-network level in children with ADHD as compared to TD children, although this was not specific to the DMN, and neither static nor time-varying WD was related to task performance. This study extends literature focusing on DMN activity or functional connectivity strength to examine DMN integration, quantified as PC, from a network topology perspective. Together, these findings indicate that higher and less variable levels of integration between DMN and task-relevant networks is related to poorer response inhibition in ADHD.

Further examination of the overall increase in integration of the DMN in ADHD revealed that significantly higher PC in ADHD was specific to DMN-FP connections. Notably, in exploratory analyses between non-DMN (task-relevant) network pairs, we additionally observed significantly greater integration between the FP-SM and FP-SUB networks in ADHD as compared to TD participants (see *Supplementary Material*). Overall, these findings indicate that while there are group-level differences in network topology in ADHD, they are likely specific to particular networks such as the DMN and FP rather than distributed evenly across the whole brain. Our findings are consistent with previous studies showing that activity and connectivity of the DMN is reliably altered in ADHD (Castellanos and Proal, 2012; Konrad and Eickhoff, 2010; Liston et al., 2011; Posner et al., 2014), including connections between DMN nodes and FP nodes (Hoekzema et al., 2014; Mills et al., 2018; Sripada et al., 2014). Few studies have examined how the FP cognitive control-related network interacts with other brain systems on a network level in ADHD, despite strong evidence for disrupted activity in top-down frontal and parietal regions associated with cognitive control (Cortese et al., 2012; Cubillo et al., 2012). The FP network is thought to underlie moment-to-moment adjustment of cognitive control (Dosenbach et al., 2008; Power and Petersen, 2013), a process probed by response control tasks such as the GNG task.

While there is a strong body of literature reporting disruptions in functional connectivity between specific fronto-parietal and subcortical regions implicated in response control in individuals with

ADHD (Castellanos and Proal, 2012; Posner et al., 2014), how the FP network interacts with cortical and subcortical networks involved in response control on the whole-network level (i.e., the SM and SUB networks) is largely unknown. We thus extend findings of altered functional connectivity in ADHD from investigating nodes of the DMN and FP networks in isolation or specific connections between networks to characterizing network topology on a larger scale between networks related to the default mode, cognitive control, and motor function.

In addition to analyses quantifying network integration (i.e., PC), we conducted exploratory analyses examining within-network coherence (i.e., WD). We observed significantly higher WD in participants with ADHD compared to TD participants, consistent with other literature reporting increased local efficiency in ADHD (Lin et al., 2014; Wang et al., 2009). Notably, there were no significant differences on an individual network level, nor were there any significant relationships between whole-network or network-level WD and behavior for either static or time-varying WD. This indicates that our findings related to network topology underlying response inhibition in ADHD are specific to across-network integration.

Our findings relating integration between the DMN and task-relevant networks to cognitive performance among children with ADHD also adds to the extant literature. We found that greater integration between the DMN and the SAL and SM networks was correlated with poorer response inhibition in children with ADHD, but not in TD children. We had hypothesized that increased DMN integration in particular would relate to poorer response control, given that DMN hyperconnectivity with other networks among individuals with ADHD is one of the most consistent findings in the literature (Castellanos et al., 2008; Hoekzema et al., 2014; Kessler et al., 2014; Mills et al., 2018; Sripada et al., 2014; Sun et al., 2012) and has been shown to relate to poorer task performance in individuals with ADHD (Fassbender et al., 2009; Helps et al., 2010; Mills et al., 2018). Our findings of increased integration between the DMN-FP networks in ADHD that was unrelated to response control, in combination with DMN-SAL and DMN-SM integration that did not differ between groups but that was correlated with response inhibition in participants with ADHD, may speak to the heterogeneity of ADHD. Specifically, DMN-FP integration (and FP integration more

broadly) may be widely observed among individuals diagnosed with ADHD, whereas DMN-SAL and DMN-SM integration may specifically relate to heterogeneity in response inhibition deficits, which are only present among a subset of children with ADHD (Nigg et al., 2005; Willcutt et al., 2005). Contrary to our predictions, DMN integration was not correlated with response variability (tau). To our knowledge, only one prior study has related network organization during the resting state to cognitive task performance among children with ADHD (Mills et al., 2018), and they did not examine response time variability. Further research is needed examining response time variability during simple attention tasks to identify the neural underpinnings of response time variability without additional task demands for response inhibition.

The brain-behavior relationships observed in the ADHD group were not found among TD participants, which is consistent with prior research examining DMN task activation and functional integration in relation to cognitive performance (Fassbender et al., 2009; Mills et al., 2018). The differential brain-behavior associations across diagnostic groups may be related to the greater cognitive demands placed on individuals with ADHD. Behaviorally, participants with ADHD performed worse on the GNG task than the TD participants (higher ComErr and tau), indicating that the task was more difficult for them and may have taxed their cognitive control and motor systems more than TD children. Research in adults has demonstrated that tasks with greater cognitive control demands result in greater network integration (Cohen and D'Esposito, 2016; Shine and Poldrack, 2018). While this study assessed network topology only during the resting state, participants were required to lie still and focus on the crosshair presented on the screen, which requires cognitive and motor control and is likely more challenging for children with ADHD. In addition, resting state network organization is theorized to recapitulate cognitive states commonly experienced by an individual (Smith et al., 2009), and studies have shown that participants perform most optimally if their resting state and task state network organization are more similar (Schultz and Cole, 2016). Perhaps the default mode, cognitive control, and motor systems are more integrated both during rest and during task performance in individuals with ADHD. Future research assessing rest-task network reconfiguration in ADHD and TD participants during tasks with differing cognitive control demands and varying difficulty levels would inform our understanding of the relationships between task demands and intrinsic functional connectivity.

In contrast to our findings of diagnostic group differences in static functional connectivity, we did not observe a group difference in time-varying functional connectivity, which is inconsistent with previous research (Abbas et al., 2019; Cai et al., 2018; de Lacy and Calhoun, 2019; Kaboodvand et al., 2020; Shappell et al., 2021; Wang et al., 2018). However, prior reports of diagnostic group differences were subtle and were observed with regard to specific subsets of networks. Our lack of group difference may be due to the specific networks included in our analyses or the different measures used (i.e., PC versus functional connectivity strength). Further, an advantage of our approach in comparison to other time-varying literature in ADHD is that we applied the DCC method to estimate network organization at each timepoint, which has been found to be more accurate than other available time-varying functional connectivity methods (Choe et al., 2017; Lindquist et al., 2014), including less susceptibility to spurious results (Hindriks et al., 2016; Laumann et al., 2017; Liégeois et al., 2017).

Despite the lack of group differences in time-varying functional connectivity, we observed that reduced CVPC between DMN and task-relevant networks was correlated with higher ComErr in children with ADHD. This suggests that less flexible network integration is related to poorer response inhibition and is consistent with one prior study reporting that increased stability of functional connections between the DMN and task-relevant networks related to poorer cognitive control (measured as increased reaction time on Stroop incongruent trials; Kaboodvand et al., 2020). Our finding that both mean PC and CVPC were

correlated with ComErr in participants with ADHD implies that underlying dynamics undetected in static analyses may have contributed to prior findings relating static DMN hyperconnectivity to increased task errors (Mills et al., 2018). To support this, our post-hoc analyses showed that CVPC explained more variance than mean PC in a regression model predicting ComErr, suggesting that combining measures of both static and time-varying functional connectivity (CVPC) provides valuable information beyond the mean PC calculated from static functional connectivity alone. Collectively, these findings support the idea that less variability/flexibility (i.e., being 'stuck' in a brain state characterized by increased interactions between the DMN and task-relevant networks) may interfere with successful cognitive control. This interpretation is consistent with theories of DMN dysfunction in ADHD postulating that fluctuations between the DMN and task-relevant networks occur intrinsically, and that disruption to these fluctuations underlies attention lapses (Sonuga-Barke and Castellanos, 2007; Weissman et al., 2006) and mind wandering (Bozhilova et al., 2018; Kucyi, 2018), both of which are increased in ADHD and may be related to each other (Bozhilova et al., 2018). However, it is important to note that there are multiple purported roles of the DMN (Andrews-Hanna et al., 2010; Buckner and DiNicola, 2019), and further research combining DMN functional connectivity variability and response time variability during task-based fMRI is needed to clarify the relationship between altered neural fluctuations reported here and in extant literature (Abbas et al., 2019; Cai et al., 2018; de Lacy and Calhoun, 2019; Kaboodvand et al., 2020) and increased behavioral fluctuations (Karalunas et al., 2014; Kofler et al., 2013; Tamm et al., 2012).

While the current study extends the existing literature examining DMN functional connectivity in relation to ADHD and deficient response control, it has some limitations. First, our sample size is relatively small, which may have limited our power to detect group differences and our ability to generalize our findings to a broader population of children with ADHD. Second, our resting state scans were relatively short (between 5.3 and 6.5 min). After scrubbing we required at least 4 min of remaining data for a participant to be included, consistent with current literature evaluating methods for optimal data processing (Parkes et al., 2018). While this scan length has been shown to be reliable (Van Dijk et al., 2010), recent studies suggest that increasing scan times increases reliability and the ability to detect individual differences in functional connectivity patterns (Gordon et al., 2017; Laumann et al., 2015). Thus, future research with longer resting state scans is important to replicate the current results. Third, it is likely there were individual differences in the cognitive processes that participants experienced during the resting state scan, and it is possible that there were group-level differences. For example, remaining still during the resting state scan may have been more effortful for the participants with ADHD, and there may have been differing levels of mind-wandering both across the groups and across participants within each group. This is a limitation of all resting state studies. Future research is needed to more fully understand individual differences in how participants experience the resting state, as well as how network organization and dynamics relate to emergent cognition (Camacho et al., 2020). Fourth, we did not match our groups for in-scanner motion given evidence that movement is correlated with ADHD symptoms, including in our sample, likely due to shared genetic factors (Couvy-Duchesne et al., 2016). However, we rigorously processed the data using 32-parameter regression, along with scrubbing for static analyses, to reduce the effects of motion and other physiological artifacts as per current recommendations (Ciric et al., 2017; Parkes et al., 2018). While scrubbing results in less data per subject, which could reduce the reliability of functional connectivity estimates, all subjects had at a minimum 4.25 min of data (102 timepoints) and the final number of volumes was not significantly different across the groups (mean ADHD = 133 volumes, mean TD = 138 volumes, $t(84) = -1.67$, $p = .10$). We additionally conducted a series of sensitivity analyses that implemented different methods of controlling for head motion (including FD and

DVARS as covariates, repeating static analyses with unscrubbed data, and including only a subgroup of participants who were matched for motion; see *Supplementary Material*). Results were largely consistent across all sensitivity analyses, suggesting that our results were unlikely to be spurious as a result of head motion (for a more nuanced discussion of findings, see *Supplementary Material* section 3.5, "Summary of Sensitivity Analysis Findings"). Due in part to our stringent motion-related inclusion criteria, we retained only 30% of our ADHD sample. In addition to reducing our sample size this may limit the generalizability of our findings, although excluded participants did not differ from analyzed participants in terms of age, sex, ADHD symptom severity, or GNG task performance. Future studies should collect resting state data of longer duration to allow for stringent motion correction while minimizing participant exclusions. As a final limitation, we used a functional brain atlas that was defined using adult data (Power et al., 2011) in our pediatric sample. While this is not optimal, this is a widely-used functional brain atlas, including in pediatric populations (e.g., Eill et al., 2019; Le et al., 2020; Marek et al., 2015; Nielsen et al., 2019; Xia et al., 2018). Future research should develop a comparable whole-brain functional atlas constructed from a pediatric sample in order to determine whether a pediatric-specific atlas would be a better fit to the data than an adult atlas.

In conclusion, using both static functional connectivity and time-varying functional connectivity we observed that increased and more stable integration between brain networks governing default mode, cognitive control, and motor function was related to poorer response inhibition in children with ADHD. This relationship was not observed in TD children. These findings expand upon existing literature that reports altered static and time-varying functional connectivity of the DMN in ADHD by observing altered network topology of the DMN, cognitive control, and motor-related networks in relation to deficient response control in children with ADHD. Collectively, this study informs our understanding of the neurobiological basis for ADHD and identifies neural mechanisms that may contribute to the heterogeneity in cognitive deficits associated with ADHD.

CRediT authorship contribution statement

Kelly A. Duffy: Data curation, Software, Formal analysis, Visualization, Writing - original draft, Writing - review & editing. **Keri S. Rosch:** Funding acquisition, Investigation, Data curation, Methodology, Formal analysis, Writing - original draft, Writing - review & editing. **Mary Beth Nebel:** Data curation, Writing - review & editing. **Karen E. Seymour:** Funding acquisition, Investigation, Data curation, Writing - review & editing. **Martin A. Lindquist:** Methodology, Software, Writing - review & editing. **James J. Pekar:** Methodology, Writing - review & editing. **Stewart H. Mostofsky:** Funding acquisition, Resources, Project administration, Investigation, Writing - review & editing. **Jessica R. Cohen:** Conceptualization, Supervision, Project administration, Data curation, Methodology, Software, Formal analysis, Visualization, Writing - original draft, Writing - review & editing.

Declaration of competing interest

One or more of the authors of this paper have disclosed potential or pertinent conflicts of interest, which may include receipt of payment, either direct or indirect, institutional support, or association with an entity in the biomedical field which may be perceived to have potential conflict of interest with this work. For full disclosure statements refer to https://doi.org/10.1016/j.dcn.2021.100980. SHM has a US patent (Patent No: US10,410,041 B2). All other authors report no biomedical financial interests or potential conflicts of interest.

Data statement

Data was collected as part of an ongoing National Institutes of Health (NIH) grant and will be made available after completion of the study as per NIH data sharing requirements.

Appendix A. Supplementary data

Supplementary material related to this article can be found online at https://doi.org/10.1016/j.dcn.2021.100980.

References

Abbas, A., Bassil, Y., Keilholz, S., 2019. Quasi-periodic patterns of brain activity in individuals with attention-deficit/hyperactivity disorder. Neuroimage: Clinical 21, 101653.

American Psychiatric Association, 2013. Diagnostic and Statistical Manual of Mental Disorders, fifth ed. American Psychiatric Publishing, Arlington, VA..

Andrews-Hanna, J.R., Reidler, J.S., Sepulcre, J., Poulin, R., Buckner, R.L., 2010. Functional-anatomic fractionation of the brain's default network. Neuron 65 (4), 550–562.

Bari, A., Robbins, T.W., 2013. Inhibition and impulsivity: behavioral and neural basis of response control. Prog. Neurobiol. 108, 44–79.

Barkley, R.A., 1997. Behavioral inhibition, sustained attention, and executive functions: constructing a unifying theory of ADHD. Psychol. Bull. 121 (1), 65–94.

Bozhilova, N.S., Michelini, G., Kuntsi, J., Asherson, P., 2018. Mind wandering perspective on attention-deficit/hyperactivity disorder. Neurosci. Biobehav. Rev. 92, 464–476.

Broyd, S.J., Demanuele, C., Debener, S., Helps, S.K., James, C.J., Sonuga-Barke, E.J.S., 2009. Default-mode brain dysfunction in mental disorders: a systematic review. Neurosci. Biobehav. Rev. 33 (3), 279–296.

Buckner, R.L., DiNicola, L.M., 2019. The brain's default network: updated anatomy, physiology and evolving insights. Nat. Rev. Neurosci. 20 (10), 593–608.

Cai, W., Chen, T., Szegletes, L., Supekar, K., Menon, V., 2018. Aberrant time-varying cross-network interactions in children with attention-deficit/hyperactivity disorder and the relation to attention deficits. Biol. Psychiatry: Cogn. Neurosci. Neuroimaging 3 (3), 263–273.

Camacho, M.C., Quiñones Camacho, L.E., Perlman, S.B., 2020. Does the child brain rest? An examination and interpretation of resting cognition in developmental cognitive neuroscience. Neuroimage 212, 116688.

Cao, M., Shu, N., Cao, Q., Wang, Y., He, Y., 2014. Imaging functional and structural brain connectomics in attention-deficit/hyperactivity disorder. Mol. Neurobiol. 50 (3), 1111–1123.

Carp, J., 2013. Optimizing the order of operations for movement scrubbing: comment on Power et al. Neuroimage 76, 436–438.

Castellanos, F.X., Aoki, Y., 2016. Intrinsic functional connectivity in attention-deficit/hyperactivity disorder: a science in development. Biol. Psychiatry Cogn. Neurosci. Neuroimaging 1 (3), 253–261.

Castellanos, F.X., Margulies, D.S., Kelly, C., Uddin, L.Q., Ghaffari, M., Kirsch, A., Shaw, D., Shehzad, Z., Di Martino, A., Biswal, B., Sonuga-Barke, E.J.S., Rotrosen, J., Adler, L.A., Milham, M.P., 2008. Cingulate-precuneus interactions: a new locus of dysfunction in adult attention-deficit/hyperactivity disorder. Biol. Psychiat. 63 (3), 6.

Castellanos, F.X., Proal, E., 2012. Large-scale brain systems in ADHD: beyond the prefrontal-striatal model. Trends Cogn. Sci. 16 (1), 17–26.

Castellanos, F.X., Sonuga-Barke, E.J.S., Scheres, A., Di Martino, A., Hyde, C., Walters, J.R., 2005. Varieties of attention-deficit/hyperactivity disorder-related intra-individual variability. Biol. Psychiat. 57 (11), 1416–1423.

Choe, A.S., Nebel, M.B., Barber, A.D., Cohen, J.R., Xu, Y., Pekar, J.J., Caffo, B., Lindquist, M.A., 2017. Comparing test-retest reliability of dynamic functional connectivity methods. Neuroimage 158, 155–175.

Ciric, R., Rosen, A.F.G., Erus, G., Cieslak, M., Adebimpe, A., Cook, P.A., Bassett, D.S., Davatzikos, C., Wolf, D.H., Satterthwaite, T.D., 2018. Mitigating head motion artifact in functional connectivity MRI. Nat. Protoc. 13 (12), 2801–2826.

Ciric, R., Wolf, D.H., Power, J.D., Roalf, D.R., Baum, G.L., Ruparel, K., Shinohara, R.T., Elliott, M.A., Eickhoff, S.B., Davatzikos, C., Gur, R.C., Gur, R.E., Bassett, D.S., Satterthwaite, T.D., 2017. Benchmarking of participant-level confound regression strategies for the control of motion artifact in studies of functional connectivity. Neuroimage 154, 174–187.

Cohen, J.R., D'Esposito, M., 2016. The segregation and integration of distinct brain networks and their relationship to cognition. J. Neurosci. 36 (48), 12083–12094.

Conners, C.K., 2002. Conners' Rating Scales-Revised. Multi-Health Systems Inc, Toronto.

Conners, C.K., 2008. Conners' 3. Multi-Health Systems Inc, North Tonawanda, NY.

Cortese, S., Kelly, C., Chabernaud, C., Proal, E., Di Martino, A., Milham, M.P., Castellanos, F.X., 2012. Toward systems neuroscience of ADHD: a meta-analysis of 55 fMRI studies. Am. J. Psychiatry 169 (10), 1038–1055.

Couvy-Duchesne, B., Ebejer, J.L., Gillespie, N.A., Duffy, D.L., Hickie, I.B., Thompson, P.M., Martin, N.G., de Zubicaray, G.I., McMahon, K.L., Medland, S.E., Wright, M.J., 2016. Head motion and inattention/hyperactivity share common genetic influences: implications for fMRI studies of ADHD. PLoS One 11 (1), e0146271.

Cubillo, A., Halari, R., Smith, A., Taylor, E., Rubia, K., 2012. A review of fronto-striatal and fronto-cortical brain abnormalities in children and adults with Attention Deficit Hyperactivity Disorder (ADHD) and new evidence for dysfunction in adults with ADHD during motivation and attention. Cortex 48 (2), 194–215.

de Lacy, N., Calhoun, V.D., 2019. Dynamic connectivity and the effects of maturation in youth with attention deficit hyperactivity disorder. Netw. Neurosci. 3 (1), 195–216.

Denckla, M.B., 1991. Attention deficit hyperactivity disorder-residual type. J. Child Neurol. 6 (Suppl), S44–50.

Dixon, M.L., Andrews-Hanna, J.R., Spreng, R.N., Irving, Z.C., Mills, C., Girn, M., Christoff, K., 2017. Interactions between the default network and dorsal attention network vary across default subsystems, time, and cognitive states. Neuroimage 147, 632–649.

Dosenbach, N.U.F., Fair, D.A., Cohen, A.L., Schlaggar, B.L., Petersen, S.E., 2008. A dual-networks architecture of top-down control. Trends Cogn. Sci. 12 (3), 99–105.

Eill, A., Jahedi, A., Gao, Y., Kohli, J.S., Fong, C.H., Solders, S., Carper, R.A., Valafar, F., Bailey, B.A., Müller, R.-A., 2019. Functional connectivities are more informative than anatomical variables in diagnostic classification of autism. Brain Connect. 9 (8), 604–612.

Esteban, O., Markiewicz, C.J., Blair, R.W., Moodie, C.A., Isik, A.I., Erramuzpe, A., Kent, J.D., Goncalves, M., DuPre, E., Snyder, M., Oya, H., Ghosh, S.S., Wright, J., Durnez, J., Poldrack, R.A., Gorgolewski, K.J., 2019. fMRIPrep: a robust preprocessing pipeline for functional MRI. Nature Methods 16 (1), 111–116.

Fair, D.A., Posner, J., Nagel, B.J., Bathula, D., Dias, T.G.C., Mills, K.L., Blythe, M.S., Giwa, A., Schmitt, C.F., Nigg, J.T., 2010. Atypical default network connectivity in youth with attention-deficit/hyperactivity disorder. Biol. Psychiat. 68 (12), 1084–1091.

Fassbender, C., Zhang, H., Buzy, W.M., Cortes, C.R., Mizuiri, D., Beckett, L., Schweitzer, J.B., 2009. A lack of default network suppression is linked to increased distractibility in ADHD. Brain Res. 1273, 114–128.

Fonov, V.S., Evans, A.C., McKinstry, R.C., Almli, C.R., Collins, D.L., 2009. Unbiased nonlinear average age-appropriate brain templates from birth to adulthood. Neuroimage 47 (Suppl 1), S102.

Gordon, E.M., Laumann, T.O., Gilmore, A.W., Newbold, D.J., Greene, D.J., Berg, J.J., Ortega, M., Hoyt-Drazen, C., Gratton, C., Sun, H., et al., 2017. Precision functional mapping of individual human brains. Neuron 95 (4), 791–807.e7.

Guimerà, R., Amaral, L.A.N., 2005a. Cartography of complex networks: modules and universal roles. J. Stat. Mech. Theory Exp. 2005 (02), P02001.

Guimerà, R., Amaral, L.A.N., 2005b. Functional cartography of complex metabolic networks. Nature 433 (7028), 895–900.

Helps, S.K., Broyd, S.J., James, C.J., Karl, A., Chen, W., Sonuga-Barke, E.J.S., 2010. Altered spontaneous low frequency brain activity in attention deficit/hyperactivity disorder. Brain Res. 1322, 134–143.

Henry, T.R., Cohen, J.R., 2019. Dysfunctional brain network organization in neurodevelopmental disorders. In: Munsell, B.C., Wu, G., Bonilha, L., Laurienti, P.J. (Eds.), Connectomics: Applications To Neuroimaging. Academic Press, San Diego, CA, pp. 83–100.

Hindriks, R., Adhikari, M.H., Murayama, Y., Ganzetti, M., Mantini, D., Logothetis, N.K., Deco, G., 2016. Can sliding-window correlations reveal dynamic functional connectivity in resting-state fMRI? Neuroimage 127, 242–256.

Hoekzema, E., Carmona, S., Ramos-Quiroga, J.A., Richarte Fernández, V., Bosch, R., Soliva, J.C., Rovira, M., Bulbena, A., Tobeña, A., Casas, M., Vilarroya, O., 2014. An independent components and functional connectivity analysis of resting state fMRI data points to neural network dysregulation in adult ADHD. Hum. Brain Mapp. 35 (4), 1261–1272.

Kaboodvand, N., Iravani, B., Fransson, P., 2020. Dynamic synergetic configurations of resting-state networks in ADHD. Neuroimage 207, 116347.

Karalunas, S.L., Geurts, H.M., Konrad, K., Bender, S., Nigg, J.T., 2014. Annual research review: reaction time variability in ADHD and autism spectrum disorders: measurement and mechanisms of a proposed trans-diagnostic phenotype. J. Child Psychol. Psychiatry 55 (6), 685–710.

Kaufman, J., Birmaher, B., Axelson, D., Perepletchikova, F., Brent, D., Ryan, N., 2013. Schedule for Affective Disorders and Schizophrenia for School-Age Children-Present and Lifetime Version (K-SADS-PL 2013, DSM-5). Western Psychiatric Institute and Yale University.

Kessler, D., Angstadt, M., Welsh, R.C., Sripada, C., 2014. Modality-spanning deficits in attention-deficit/hyperactivity disorder in functional networks, gray matter, and white matter. J. Neurosci. 34 (50), 16555–16566.

Kofler, M.J., Rapport, M.D., Sarver, D.E., Raiker, J.S., Orban, S.A., Friedman, L.M., Kolomeyer, E.G., 2013. Reaction time variability in ADHD: a meta-analytic review of 319 studies. Clin. Psychol. Rev. 33 (6), 795–811.

Konrad, K., Eickhoff, S.B., 2010. Is the ADHD brain wired differently? A review on structural and functional connectivity in attention deficit hyperactivity disorder. Hum. Brain Mapp. 31 (6), 904–916.

Kucyi, A., 2018. Just a thought: how mind-wandering is represented in dynamic brain connectivity. Neuroimage 180 (Pt B), 505–514.

Kucyi, A., Hove, M.J., Esterman, M., Hutchison, R.M., Valera, E.M., 2017. Dynamic brain network correlates of spontaneous fluctuations in attention. Cerebral Cortex 27 (3), 1831–1840.

Lacouture, Y., Cousineau, D., 2008. How to use MATLAB to fit the ex-Gaussian and other probability functions to a distribution of response times. Tutor. Quant. Methods Psychol. 4 (1), 35–45.

Laumann, T.O., Gordon, E.M., Adeyemo, B., Snyder, A.Z., Joo, S.J., Chen, M.-Y., Gilmore, A.W., McDermott, K.B., Nelson, S.M., Dosenbach, N.U., et al., 2015. Functional system and areal organization of a highly sampled individual human brain. Neuron 87 (3), 657–670.

Laumann, T.O., Snyder, A.Z., Mitra, A., Gordon, E.M., Gratton, C., Adeyemo, B., Gilmore, A.W., Nelson, S.M., Berg, J.J., Greene, D.J., McCarthy, J.E., Tagliazucchi, E., Laufs, H., Schlaggar, B.L., Dosenbach, N.U.F., Petersen, S.E., 2017. On the stability of BOLD fMRI correlations. Cerebral Cortex 27 (10), 4719–4732.

Le, T.M., Huang, A.S., O'Rawe, J., Leung, H.-C., 2020. Functional neural network configuration in late childhood varies by age and cognitive state. Dev. Cogn. Neurosci. 45, 100862.

Leth-Steensen, C., Elbaz, Z.K., Douglas, V.I., 2000. Mean response times, variability, and skew in the responding of ADHD children: a response time distributional approach. Acta Psychol. 104 (2), 167–190.

Liégeois, R., Laumann, T.O., Snyder, A.Z., Zhou, H.J., Yeo, B., 2017. Interpreting temporal fluctuations in resting-state functional connectivity MRI. Neuroimage 163, 437–455.

Lijffijt, M., Kenemans, J.L., Verbaten, M.N., van Engeland, H., 2005. A meta-analytic review of stopping performance in attention-deficit/hyperactivity disorder: deficient inhibitory motor control? J. Abnormal Psychol. 114 (2), 216–222.

Lin, P., Sun, J., Yu, G., Wu, Y., Yang, Y., Liang, M., Liu, X., 2014. Global and local brain network reorganization in attention-deficit/hyperactivity disorder. Brain Imaging Behav. 8 (4), 558–569.

Lindquist, M.A., Geuter, S., Wager, T.D., Caffo, B.S., 2019. Modular preprocessing pipelines can reintroduce artifacts into fMRI data. Hum. Brain Mapp. 40 (8), 2358–2376.

Lindquist, M.A., Xu, Y., Nebel, M.B., Caffo, B.S., 2014. Evaluating dynamic bivariate correlations in resting-state fMRI: a comparison study and a new approach. Neuroimage 101, 531–546.

Liston, C., Malter Cohen, M., Teslovich, T., Levenson, D., Casey, B.J., 2011. Atypical prefrontal connectivity in attention-deficit/hyperactivity disorder: pathway to disease or pathological end point? Biol. Psychiat. 69 (12), 1168–1177.

Marek, S., Hwang, K., Foran, W., Hallquist, M.N., Luna, B., 2015. The contribution of network organization and integration to the development of cognitive control. PLoS Biol. 13 (12), e1002328.

Mills, B.D., Miranda-Dominguez, O., Mills, K.L., Earl, E., Cordova, M., Painter, J., Karalunas, S.L., Nigg, J.T., Fair, D.A., 2018. ADHD And attentional control: impaired segregation of task positive and task negative brain networks. Netw. Neurosci. 2 (2), 200–217.

Mostofsky, S.H., Simmonds, D.J., 2008. Response inhibition and response selection: two sides of the same coin. J. Cogn. Neurosci. 20 (5), 751–761.

Nielsen, A.N., Greene, D.J., Gratton, C., Dosenbach, N.U.F., Petersen, S.E., Schlaggar, B.L., 2019. Evaluating the prediction of brain maturity from functional connectivity after motion artifact denoising. Cerebral Cortex 29 (6), 2455–2469.

Nigg, J.T., Willcutt, E.G., Doyle, A.E., Sonuga-Barke, E.J.S., 2005. Causal heterogeneity in attention-deficit/hyperactivity disorder: do we need neuropsychologically impaired subtypes? Biol. Psychiat. 57 (11), 1224–1230.

Parkes, L., Fulcher, B., Yücel, M., Fornito, A., 2018. An evaluation of the efficacy, reliability, and sensitivity of motion correction strategies for resting-state functional MRI. Neuroimage 171, 415–436.

Posner, J., Park, C., Wang, Z., 2014. Connecting the dots: a review of resting connectivity MRI studies in attention-deficit/hyperactivity disorder. Neuropsychol. Rev. 24 (1), 3–15.

Power, J.D., Cohen, A.L., Nelson, S.M., Wig, G.S., Barnes, K.A., Church, J.A., Vogel, A.C., Laumann, T.O., Miezin, F.M., Schlaggar, B.L., Petersen, S.E., 2011. Functional network organization of the human brain. Neuron 72 (4), 665–678.

Power, J.D., Mitra, A., Laumann, T.O., Snyder, A.Z., Schlaggar, B.L., Petersen, S.E., 2014. Methods to detect, characterize, and remove motion artifact in resting state fMRI. Neuroimage 84, 320–341.

Power, J.D., Petersen, S.E., 2013. Control-related systems in the human brain. Curr. Opin. Neurobiol. 23 (2), 223–228.

Raichle, M.E., MacLeod, A.M., Snyder, A.Z., Powers, W.J., Gusnard, D.A., Shulman, G.L., 2001. A default mode of brain function. Proc. Natl. Acad. Sci. USA 98 (2), 676–682.

Reich, W., Welner, Z., Herjanic, B., 1997. Diagnostic Interview for Children and Adolescents-IV. Multi-Health Systems Inc, Toronto.

Rubinov, M., Sporns, O., 2010. Complex network measures of brain connectivity: uses and interpretations. Neuroimage 52 (3), 1059–1069.

Sadaghiani, S., Poline, J.B., Kleinschmidt, A., D'Esposito, M., 2015. Ongoing dynamics in large-scale functional connectivity predict perception. Proc. Natl. Acad. Sci. USA 112 (27), 8463–8468.

Schultz, D.H., Cole, M.W., 2016. Higher intelligence is associated with less task-related brain network reconfiguration. J. Neurosci. 36 (33), 8551–8561.

Sergeant, J.A., 2005. Modeling attention-deficit/hyperactivity disorder: a critical appraisal of the cognitive-energetic model. Biol. Psychiat. 57 (11), 1248–1255.

Shappell, H.M., Duffy, K.A., Rosch, K.S., Pekar, J.J., Mostofsky, S.H., Lindquist, M.A., Cohen, J.R., 2021. Children with attention-deficit/hyperactivity disorder spend more time in hyperconnected network states and less time in segregated network states as revealed by dynamic connectivity analysis. Neuroimage 229, 117753.

Shine, J.M., Poldrack, R.A., 2018. Principles of dynamic network reconfiguration across diverse brain states. Neuroimage 180 (Pt B), 396–405.

Smith, S.M., Fox, P.T., Miller, K.L., Glahn, D.C., Fox, P.M., Mackay, C.E., Filippini, N., Watkins, K.E., Toro, R., Laird, A.R., Beckmann, C.F., 2009. Correspondence of the brain's functional architecture during activation and rest. Proc. Natl. Acad. Sci. USA 106 (31), 13040–13045.

Sonuga-Barke, E.J.S., Castellanos, F.X., 2007. Spontaneous attentional fluctuations in impaired states and pathological conditions: a neurobiological hypothesis. Neurosci. Biobehav. Rev. 31 (7), 977–986.

Sripada, C., Kessler, D., Fang, Y., Welsh, R.C., Prem. Kumar, K., Angstadt, M., 2014. Disrupted network architecture of the resting brain in attention-deficit/hyperactivity disorder. Hum. Brain Mapp. 35 (9), 4693–4705.

Sun, L., Cao, Q., Long, X., Sui, M., Cao, X., Zhu, C., Zuo, X., An, L., Song, Y., Zang, Y., Wang, Y., 2012. Abnormal functional connectivity between the anterior cingulate and the default mode network in drug-naïve boys with attention deficit hyperactivity disorder. Psychiatry Res. 201 (2), 120–127.

Tamm, L., Narad, M.E., Antonini, T.N., O'Brien, K.M., Hawk, L.W., Epstein, J.N., 2012. Reaction time variability in ADHD: a review. Neurotherapeutics 9 (3), 500–508.

van den Heuvel, M.P., de Lange, S.C., Zalesky, A., Seguin, C., Yeo, B.T.T., Schmidt, R., 2017. Proportional thresholding in resting-state fMRI functional connectivity networks and consequences for patient-control connectome studies: issues and recommendations. Neuroimage 152, 437–449.

Van Dijk, K.R.A., Hedden, T., Venkataraman, A., Evans, K.C., Lazar, S.W., Buckner, R.L., 2010. Intrinsic functional connectivity as a tool for human connectomics: theory, properties, and optimization. J. Neurophysiol. 103 (1), 297–321.

Wang, X.-H., Jiao, Y., Li, L., 2018. Identifying individuals with attention deficit hyperactivity disorder based on temporal variability of dynamic functional connectivity. Sci. Rep. 8 (1), 11789.

Wang, L., Zhu, C., He, Y., Zang, Y., Cao, Q., Zhang, H., Zhong, Q., Wang, Y., 2009. Altered small-world brain functional networks in children with attention-deficit/hyperactivity disorder. Hum. Brain Mapp. 30 (2), 638–649.

Wechsler, D., 2002. Wechsler Individual Achievement Test (WIAT-II), second ed. Psychological Corporation, San Antonio, TX.

Wechsler, D., 2003. Wechsler Intelligence Scale for Children (WISC-IV), fourth ed. Psychological Corporation, San Antonio, TX.

Wechsler, D., 2009. Wechsler Individual Achievement Test (WIAT-III), third ed. Pearson, San Antonio, TX.

Wechsler, D., 2014. Wechsler Intelligence Scale for Children (WISC-V), fifth ed. Pearson, Bloomington, MN.

Weissman, D.H., Roberts, K.C., Visscher, K.M., Woldorff, M.G., 2006. The neural bases of momentary lapses in attention. Nature Neurosci. 9 (7), 971–978.

Willcutt, E.G., Doyle, A.E., Nigg, J.T., Faraone, S.V., Pennington, B.F., 2005. Validity of the executive function theory of attention-deficit/hyperactivity disorder: a meta-analytic review. Biol. Psychiat. 57 (11), 1336–1346.

Xia, C.H., Ma, Z., Ciric, R., Gu, S., Betzel, R.F., Kaczkurkin, A.N., Calkins, M.E., Cook, P.A., García de la Garza, A., Vandekar, S.N., et al., 2018. Linked dimensions of psychopathology and connectivity in functional brain networks. Nature Commun. 9 (1), 3003.